Dalton Transactions

PAPER

View Article Online
View Journal | View Issue

Cite this: *Dalton Trans.*, 2014, **43**, 4962

Radical coupling for directed C–C/C–S bond formation in the reaction of $Cp^*IrS_2C_2B_{10}H_{10}$ with 1-azido-3-nitrobenzene†

Wei Zhong,[a,b] Qibai Jiang,[a] Qian Zhang,[a] Yi Shang,[a] Hong Yan*[a] and Vladimir Bregadze*[c]

Received 22nd August 2013,
Accepted 23rd September 2013

DOI: 10.1039/c3dt52308j

www.rsc.org/dalton

Reactions of half-sandwich complex $Cp^*IrS_2C_2B_{10}H_{10}$ (**1**) with 1-azido-3-nitrobenzene (3-$NO_2C_6H_4N_3$, **L**) upon heating or under light led to new complexes **2–6**. Complexes **2** and **3** contain a five-membered cyclometalated ligand arising from C(sp^2)–H activation of the azide ligand **L**. Complex **4** is a 16 electron species containing a new-generated C–C bond between the azide ligand **L** and the Cp* unit where C(sp^3)–H activation of the methyl unit occurred. Complexes **5** and **6** contain two types of the ligand which appear in complexes **2**, **3** and **4**. Further reactions of complexes **5** and **6** with **L** under more harsh conditions gave rise to the nucleophilic addition products **7** and **8**, where ring expansion of the azide ligand at the imido site of complexes **5** and **6** happened. Complexes **2–8** were characterized by NMR, MS, IR, and elemental analysis, and X-ray structural analyses were performed for complexes **2–4** and **6–8**. The radical mechanisms for the formation of complexes **2–6** were proposed on the basis of capture experiments by EPR and ESI-MS. And the formation mechanism of complexes **7** and **8** was also suggested.

Introduction

Aryl nitrenes, which are readily available from the photolysis or thermolysis of aryl azides, are among the most thoroughly investigated reactive intermediates.[1–4] Present studies of aryl nitrenes are focused on the organic system, such as photochemistry of phenyl azide.[5–8] Comparatively, nitrene chemistry in the organometallic field is much less explored, although organic azides were used extensively for the preparation of imido complexes and organoazido metal complexes.[9–11] Among a few reported examples, Abu-Omar and co-workers described a novel mechanism for the reactions of aryl azides with manganese corroles in which the metal captures triplet nitrene rather than form an organoazido complex;[12] Bruin *et al.* presented EPR spectroscopic and detailed computational study on the Co(por)-catalyzed amination of benzylic C–H bonds by different organic azides, which proceed *via* a multistep radical mechanism involving an unusual "nitrene radical" intermediate (por)Co^{III}–N·Y;[13] Peters reported facile catalytic N–N coupling of aryl azides to yield azoarenes mediated by the Ru(I) metalloradical [SiP^{iPr}_3]Ru(N_2).[14] On the other hand, it is well-established that photolysis or thermolysis of aryl azides initially yields singlet aryl nitrenes, which then either undergo intersystem crossing to the triplet ground state or rearrange to didehydroazepines *via* bicyclic azirines.[5,15–18] Among these sequential transformations, we assumed that addition of an appropriate metal complex may capture some reactive intermediates or lead to some unexpected results. Bearing this in mind and considering the activity of the 16-electron half-sandwich complex $Cp^*IrS_2C_2B_{10}H_{10}$ (**1**) with different substrates,[19] our recent study on the thermal and photochemical reactions of complex **1** with 2,6-disubstituted aryl azides showed C(sp^3)–H activation and electron-withdrawing group migration.[20] To further understand such transformations and explore the scope of organic azides, we focus on the reactions of other aryl azides with complex **1**. In this paper, we report on the reaction of **1** and 1-azido-3-nitrobenzene (**L**) which has led to C–C and/or C–S bond formation *via* radical coupling initiated by heat or light.

[a]*State Key Laboratory of Coordination Chemistry, School of Chemistry and Chemical Engineering, Nanjing University, Nanjing, Jiangsu 210093, China. E-mail: hyan1965@nju.edu.cn; Tel: +86-25-83686724*
[b]*College of Biological, Chemical Sciences and Engineering, Jiaxing University, Jiaxing, Zhejiang 314001, China. Tel: +86-573-83640303*
[c]*A. N. Nesmeyanov Institute of Organoelement Compounds (INEOS), Russian Academy of Sciences, Vavilov Str. 28, Moscow, 119991, Russia. E-mail: bre@ineos.ac.ru; Tel: +7-499-135-7405*
†CCDC 936371–936376. For crystallographic data in CIF or other electronic format see DOI: 10.1039/c3dt52308j

Results and discussion

Reaction of complex 1 and 3-$NO_2C_6H_4N_3$ (L)

Similar to the reactions of **1** with 2,6-disubstituted aryl azides that we previously investigated,[20] cyclometalated complexes **2** and **3** were formed as expected in the reaction of **1** with excess **L** upon heating in toluene (80 °C) (Scheme 1). Two additional products **5** and **6** were also isolated from this reaction in yields of 14.5% and 15.8%, respectively. It is not surprising that two *ortho*-positions in **L** have the same possibility for cyclometalation and the results gave the two expected types of products **2** and **3** with a ratio of 2/3. But interestingly, another product **4** was obtained if treated with one equiv. or less **L** in the reaction. If excess **L** was used, complex **4** could not be isolated as it further reacted with ligand to produce **5** and **6** in moderate yields. Note that the further reactions of complexes **2** and **3** with excess **L** did not lead to **5** and **6**, but products **7** and **8**, respectively, under higher temperature or longer photolysis (Scheme 1).

Characterization of complexes 2–8

All these complexes were fully characterized by NMR spectroscopy, mass spectrometry, and elemental analysis. Additionally, the solid state structures of these complexes were solved by X-ray crystallography with the exception of complex **5**.

Crystal structures of **2** and **3** are shown in Fig. 1. As two isomeric examples, the common feature of both is the covalent combination of one sulfur atom with an *ortho*-position carbon atom of the phenyl ring to construct a five-membered Ir–N–C–C–S metallacyclic ring, which shares one Ir–S bond with the original five-membered ring in complex **1** (Ir–S–C–C–S). In each case the new "SSN" pincer ligand derived from the azide and carboranyl dithiolate, is coordinated to the iridium center *via* Ir–S/Ir←S/Ir–N bonding. Although structurally similar to reported alkyne-inserted 18-electron adducts,[21–24] the formation of the Ir–N–C–C–S ring within **2** and **3** can be inferred as a different pathway because of the necessary activation of a C–H bond of

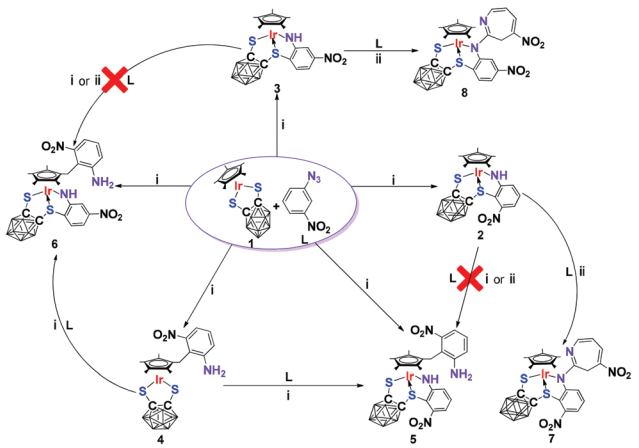

Scheme 1 The synthesis of complexes **2–8**. Reaction conditions: (i) toluene, 80 °C, 3 hours or *hν*, RT, 30 minutes; (ii) toluene, reflux, 24 hours or *hν*, RT, 3 hours.

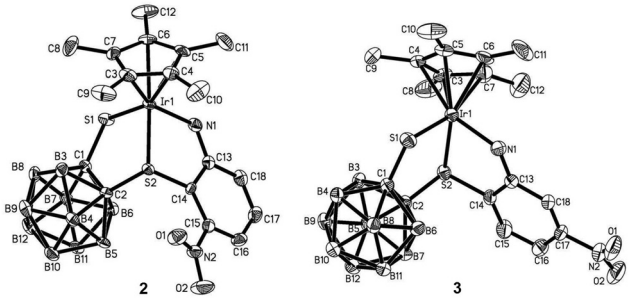

Fig. 1 Molecular structures of **2** and **3** with 30% displacement ellipsoids. All H atoms are omitted for clarity.

the phenyl (*ortho*-position) ring. The C13–N1 lengths in **2** and **3** are 1.349 and 1.330 Å, respectively, demonstrating a feature of a double bond, close to the cyclometallated amino-carbene complexes.[25] This is also consistent with the Ir1–N1–C13 bond angle of 120–122°, indicative of sp^2 hybridization of the N1 atom. The characteristic –NH signals in the ^{1}H NMR spectra of complexes **2** and **3** are assigned to the broad singlets at 4.30 ppm and 4.13 ppm, respectively. Three phenyl proton resonances, which show two doublets and one triplet in **2** and one singlet and two doublets in **3**, are supportive of cyclometalation in these complexes.

The molecular structure of **4** (Fig. 2) inherits the $[IrS_2C_2B_{10}H_{10}]$ moiety from the precursor **1**, but with a new ancillary ligand which is generated from the coupling of Cp* ligand with aryl azide. Therein, the carbon atom between nitro and azido groups connects with one methyl group of Cp* and the nitrogen is subsequently converted to the NH_2 group *via* hydrogen transfer after the loss of N_2. In comparison to the formation of complexes **2** and **3**, it appears that complex **4** adopts a different pathway from the 16-electron precursor **1** and azide. Consistent with the solid structure, the ^{1}H NMR spectrum showed one broad signal at 4.55 ppm ascribed to the $-NH_2$ group, one singlet at 3.51 ppm assigned to the methylene group and two singlets at 1.87 and 1.76 ppm assigned to four methyl groups. The ^{13}C NMR signal for methylene appears at 25.77 ppm whereas the methyl signals appear as two close singlets at 9.83 and 10.13 ppm.

A perspective view of complex **6** is shown in Fig. 2. The structure of **6** can be considered as the combination of **3** and

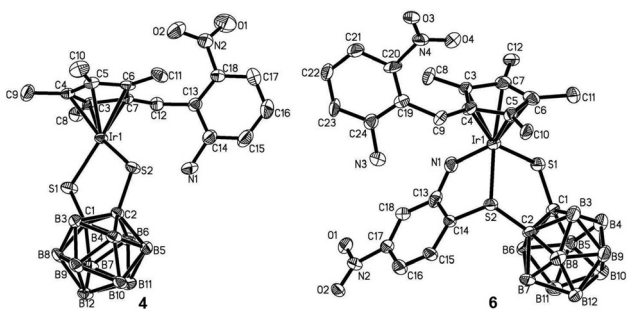

Fig. 2 Molecular structures of **4** and **6** with 30% displacement ellipsoids. All H atoms are omitted for clarity.

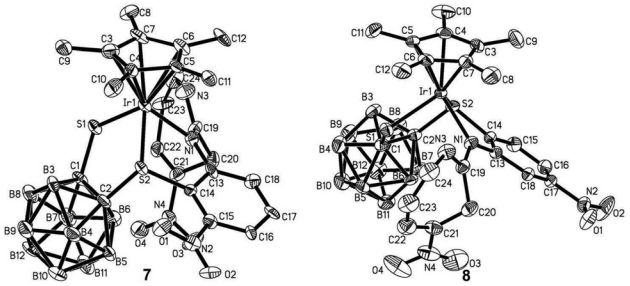

Fig. 3 Molecular structures of **7** and **8** with 30% displacement ellipsoids. All H atoms are omitted for clarity.

4, with the same cyclometalation in **3** and C–H activation of the Cp* ligand in **4**. But its ^{1}H NMR spectrum shows some differences from **4**, with two doublets at 3.59 and 3.70 ppm (J = 17 Hz) due to the diastereotopic protons of the methylene group and four singlets in the range of 1.51–1.84 ppm for the inequivalent methyl groups. The NMR spectra of **5** are similar to those of **6**, with the main difference in the phenyl signals of cyclometalation, thus supporting the proposed structure.

The molecular structures of **7** and **8** are shown in Fig. 3. Both complexes **7** and **8** demonstrate that the nitrogen atom in the five-membered Ir–N–C–C–S metallacyclic ring is bound to a distorted seven-membered heterocycle, which is named as 4-nitro-3*H*-azepine. Complexes **7** and **8** can be thought of as the nucleophilic addition of **2** and **3** with **L** after the loss of N_2 and ring expansion. With the same skeleton of the Ir–N–C–C–S metallacyclic ring sharing one Ir–S bond with the original five-membered ring Ir–S–C–C–S in **2** and **3**, the Ir1–N1 and N1–C13 lengths in **7** and **8** are 0.09 Å and 0.05 Å longer than those in **2** and **3** on average. All other distances and angles are in the expected range. The ^{1}H NMR spectra show the signals of Cp*, phenyl and 4-nitro-3*H*-azepine in rational regions. The resonances at δ = 1.27 ppm are attributed to the CH_2 groups in the 4-nitro-3*H*-azepine of both complexes **7** and **8**, whose corresponding ^{13}C NMR signals appear at δ = 32.99 and 32.19 ppm, respectively.

Mechanistic considerations

Generally, the interaction between transition metal complexes and organic azides usually undergoes two plausible pathways: one proceeds in an ionic reaction *via* dipolar addition to the substrates; the other forms nitrene species and then reacts further to give a variety of products, which in some cases involve radical intermediates and undergo a radical mechanism. As shown above, the reactions demonstrate unusual C–H activation in phenyl/methyl to form C–S and C–C bonds. This inspired us to consider a radical mechanism. For mechanistic elucidation, EPR experiments were carried out. *In situ* irradiation of the solution of **1**, **L** and the radical capture reagent, 5,5-dimethyl-1-pyrroline *N*-oxide (DMPO), strong EPR signals were observed (Fig. 4). More than this, the DMPO/radical adducts could be detected by ESI-MS after irradiation for two minutes (Fig. 5). The peak at m/z 782.83 corresponds to [**1** + **L**-N_2 + DMPO] species, and the peak at m/z 982.25 matches the formula [**1** + 2**L**-2N_2 + DMPO + Na + MeCN + H^+]. Nevertheless, the results of EPR signal change with irradiation time indicate that the DMPO/radical adducts can survive within 40 minutes (Fig. 4), thus the DMPO/radical adducts are hard to be isolated and further characterized. The lower percentages of the peaks at m/z 782.83 and 982.25 in ESI-MS spectra also reflect the instability of the DMPO/radical adducts (Fig. 5). For comparison, the reaction was also conducted under photolytic conditions, lower yields of expected compounds were isolated than under thermal conditions.

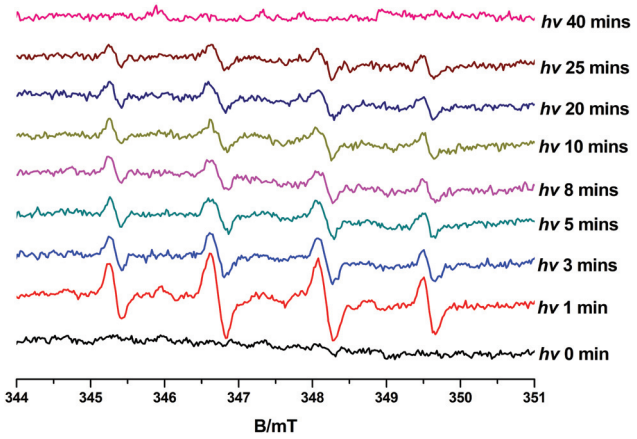

Fig. 4 EPR spectra (X band, 9.7 GHz, room temperature) for reaction mixtures in the different periods of irradiation: the radical trap agent DMPO (100 mM), **1** (100 mM) and **L** (100 mM).

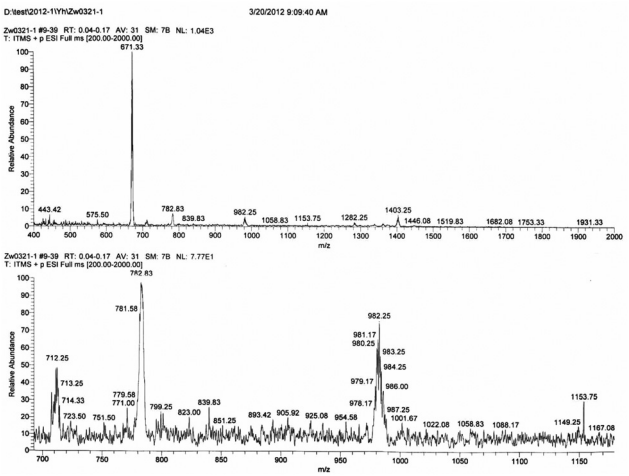

Fig. 5 ESI-MS spectra of the mixture of DMPO (100 mM), **1** (100 mM) and **L** (100 mM) after irradiation for two minutes without any workup.

Based on the above experiments, a plausible mechanism involving radical species for the formation of compounds **2–6** is proposed in Scheme 2. In the first step, azide ligand **L** interacting with 16-electron species **1** to generate metal–imido complex **I** is suggested. This species can transform into diradical **II**, then to **IIIA–IIIC** by hydrogen abstraction and radical

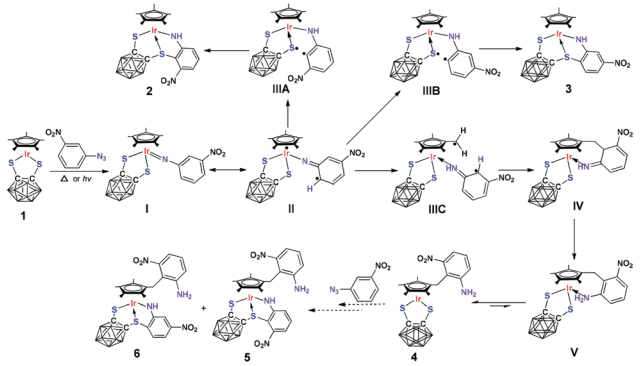

Scheme 2 Proposed mechanisms for the formation of complexes **2–6**.

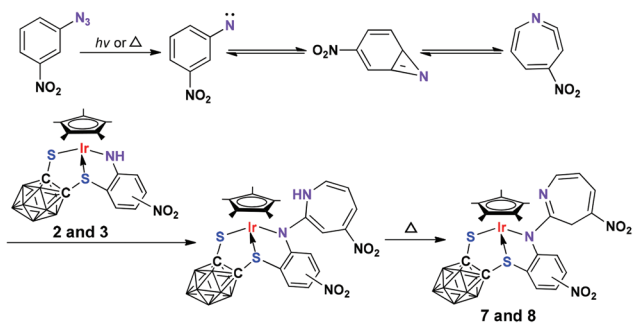

Scheme 3 The formation of complexes **7** and **8**.

migration.[26] After these processes intramolecular radical coupling happens to lead to products **2** and **3**. Similarly, intermediate **IV**, which is supported and evidenced by the analogous product in our previous report,[20] is formed by intramolecular radical coupling of **IIIC** in the same way. In this case, **IV** may be thermodynamically unstable and may rearrange to amino-coordinated species **V**, which can easily transform to compound **4** due to the weak coordination of the amino group. The formation of compounds **5** and **6** repeat the same pathway as the formation of complexes **2** and **3** from **1** and **L**.

On the other hand, photolysis or thermolysis of phenyl azide has been studied extensively[5,16,17] and it is well conceivable that such processes yield phenylnitrene, which acts as a singlet species and undergoes ring expansion. The first step is to form a bicyclic azepine intermediate, then further rearrange to a seven-membered ring keteneimine product, which may be trapped by nucleophiles (*e.g.* Et_2NH). In our case, the formation of **7** and **8** can be regarded as the –NH group in **2** and **3** acting as a nucleophile to add to the seven-membered heterocycle 4-nitro-3*H*-azepine, which is formed from ring expansion and rearrangement of initial azide ligand **L** (Scheme 3).

Conclusions

We have shown that thermal and photolytic reaction of half-sandwich complex **1** and 1-azido-3-nitrobenzene led to new products involving C–C and C–S bond formation *via* C–H activation undergoing a radical mechanism. The unsaturated characterization of complex **1** together with the nature of azide ligand **L** is responsible for such interesting chemical transformation. We also found that the –NH group in metal complexes can act as a nucleophile to trap the seven-membered ring keteneimine in nitrene chemistry. The preliminary results have shown application potential in organometallic or organic synthesis.

Experimental

Compounds were prepared and handled by standard Schlenk techniques. Toluene was predried over molecular sieves and distilled over CaH_2 under nitrogen prior to use. $Cp^*IrS_2C_2B_{10}H_{10}$ (**1**)[27] and 1-azido-3-nitrobenzene[28] were prepared by literature procedures. The NMR measurements were performed using a Bruker DRX 500 spectrometer. Chemical shifts were given with respect to $CHCl_3/CDCl_3$ (δ ^{1}H = 7.24 ppm; δ ^{13}C = 77.0 ppm) and external $Et_2O{\cdot}BF_3$ (δ ^{11}B = 0 ppm). The IR spectra were recorded using a Bruker Vector 22 spectrophotometer with KBr pellets in the region of 4000–400 cm^{-1}. The C, H and N microanalyses were carried out with an Elementar Vario EL III elemental analyzer. Mass data were determined with the LCQ (ESI-MS, Thermo Finnigan) mass spectrometer.

Preparation of complexes 2–6

The mixture of complex **1** (106.8 mg, 0.2 mmol) and 1-azido-3-nitrobenzene (0.2 or 1.0 mmol) was heated at 80 °C in dried toluene for 3 hours. The solvent was removed and the crude product was purified by chromatography using silica gel. (Note: complex **4** was obtained when one equivalent 1-azido-3-nitrobenzene was used.)

2 (16.8 mg, 12.5%). Purple solid. ^{1}H NMR: 7.06 (d, J = 7.0 Hz, 1H, Ar*H*), 6.97 (t, J = 7.5 Hz, 1H, Ar*H*), 6.86 (d, J = 7.0 Hz, 1H, Ar*H*), 4.30 (s, 1H, N*H*), 1.80 (s, 15H, CH_3, Cp*). ^{11}B{^{1}H} NMR: −1.7 (2B), −3.1 (2B), −4.4 (2B), −6.9 (2B), −8.1 (1B), −8.8 (1B). ^{13}C NMR: 8.59 (CH_3, Cp*), 90.02 (carborane), 93.27 (C, Cp*), 103.05 (C, Ph), 108.85 (carborane), 110.16 (CH, Ph), 123.38 (CH, Ph), 132.54 (CH, Ph), 149.69 (C, Ph), 167.30 (C, Ph). ESI-MS (m/z): 669.17 (100%) $[M]^-$. IR (KBr, cm^{-1}): 2565.8 (ν_{B-H}). Anal. Found: C, 32.03; H, 4.49; N, 4.03. Calcd for $C_{18}H_{29}B_{10}IrN_2O_2S_2$: C, 32.27; H, 4.36; N, 4.18.

3 (26.3 mg, 19.6%). Purple solid. ^{1}H NMR: 7.38 (s, 1H, Ar*H*), 7.30 (d, J = 8.5 Hz, 1H, Ar*H*), 6.93 (d, J = 8.5 Hz, 1H, Ar*H*), 4.13 (s, 1H, N*H*), 1.79 (s, 15H, CH_3, Cp*). ^{11}B{^{1}H} NMR: −1.4 (2B), −2.7 (2B), −4.9 (2B), −6.9 (2B), −8.0 (1B), −9.7 (1B). ^{13}C NMR: 8.61 (CH_3, Cp*), 89.17 (carborane), 93.19 (C, Cp*), 105.08 (CH, Ph), 106.78 (carborane), 110.49 (CH, Ph), 116.62 (C, Ph), 134.42 (CH, Ph), 151.83 (C, Ph), 164.34 (C, Ph). ESI-MS (m/z): 669.33 (100%) $[M]^-$. IR (KBr, cm^{-1}): 2586.7 (ν_{B-H}). Anal. Found: C, 31.92; H, 4.21; N, 4.27. Calcd for $C_{18}H_{29}B_{10}IrN_2O_2S_2$: C, 32.27; H, 4.36; N, 4.18.

4 (23.6 mg, 17.6%). Bluish green solid. ^{1}H NMR: 7.34 (d, J = 8.0 Hz, 1H, Ar*H*), 7.26 (t, J = 8 Hz, 1H, Ar*H*), 6.98 (d, J = 8 Hz,

1H, Ar*H*), 4.45 (s, 2H, NH_2), 3.51 (s, 2H, CH_2, Cp*), 1.87 (s, 6H, 2 × CH_3, Cp*), 1.76 (s, 6H, 2 × CH_3, Cp*). $^{11}B\{^1H\}$ NMR: −3.5 (1B), −4.7 (3B), −5.5 (3B), −6.9 (3B). ^{13}C NMR: 9.83 (2 × CH_3, Cp*), 10.13 (2 × CH_3, Cp*), 25.77 (CH_2, Cp*), 91.22 (CCH_2, Cp*), 92.02 (carborane), 92.35 (2 × CCH_3, Cp*), 93.24 (2 × CCH_3, Cp*), 113.53 (C, Ph), 114.63 (CH, Ph), 120.88 (CH, Ph), 129.01 (CH, Ph), 147.40 (C, Ph), 151.37 (C, Ph). ESI-MS (*m*/*z*): 671.67 (100%) $[M + H^+]^+$. IR (KBr, cm^{-1}): 2579.2 (ν_{B-H}). Anal. Found: C, 32.10; H, 4.25; N, 3.97. Calcd for $C_{18}H_{29}B_{10}IrN_2O_2S_2$: C, 32.27; H, 4.36; N, 4.18.

5 (23.4 mg, 14.5%). Light brown solid. ^1H NMR: 7.30 (d, *J* = 7.5 Hz, 1H, Ar*H*), 7.22 (t, *J* = 8.0 Hz, 1H, Ar*H*), 7.11 (d, *J* = 7.5 Hz, 1H, Ar*H*), 7.02 (t, *J* = 8.0 Hz, 1H, Ar*H*), 6.92 (d, *J* = 7.5 Hz, 1H, Ar*H*), 6.90 (d, *J* = 7.5 Hz, 1H, Ar*H*), 4.42 (s, 2H, NH_2), 4.34 (s, 1H, N*H*), 3.73 (d, *J* = 17.0 Hz, 1H, CH*H*), 3.62 (d, *J* = 17.0 Hz, 1H, C*H*H), 1.84 (s, 3H, CH_3, Cp*), 1.77 (s, 3H, CH_3, Cp*), 1.71 (s, 3H, CH_3, Cp*), 1.56 (s, 3H, CH_3, Cp*). $^{11}B\{^1H\}$ NMR: −1.6 (2B), −2.8 (2B), −4.3 (3B), −6.8 (2B), −8.3 (1B). ^{13}C NMR: 8.32 (CH_3, Cp*), 8.82 (CH_3, Cp*), 9.02 (CH_3, Cp*), 9.17 (CH_3, Cp*), 21.99 (CH_2, Cp*), 89.15 (carborane), 92.68 (C, Cp*), 92.93 (C, Cp*), 93.25 (C, Cp*), 94.08 (C, Cp*), 95.63 (C, Cp*), 103.02 (C, Ph), 108.18 (carborane), 110.57 (CH, Ph), 114.12 (C, Ph), 114.57 (CH, Ph), 120.30 (CH, Ph), 123.47 (CH, Ph), 128.63 (CH, Ph), 132.79 (CH, Ph), 147.24 (C, Ph), 149.62 (C, Ph), 151.13 (C, Ph), 167.25 (C, Ph). ESI-MS (*m*/*z*): 805.25 (100%) $[M]^-$. IR (KBr, cm^{-1}): 2587.6 (ν_{B-H}). Anal. Found: C, 35.42; H, 4.25; N, 6.81. Calcd for $C_{24}H_{33}B_{10}IrN_4O_4S_2$: C, 35.76; H, 4.13; N, 6.95.

6 (25.5 mg, 15.8%). Brown solid. ^1H NMR: 7.41 (s, 1H, Ar*H*), 7.30 (d, *J* = 8.5 Hz, 1H, Ar*H*), 7.28 (t, *J* = 8.0 Hz, 1H, Ar*H*), 7.22 (t, *J* = 8.0 Hz, 1H, Ar*H*), 6.98 (d, *J* = 7.5 Hz, 1H, Ar*H*), 6.93 (d, *J* = 7.5 Hz, 1H, Ar*H*), 4.39 (s, 2H, NH_2), 4.24 (s, 1H, N*H*), 3.70 (d, *J* = 17.0 Hz, 1H, CH*H*), 3.59 (d, *J* = 17.0 Hz, 1H, C*H*H), 1.84 (s, 3H, CH_3, Cp*), 1.78 (s, 3H, CH_3, Cp*), 1.70 (s, 3H, CH_3, Cp*), 1.51 (s, 3H, CH_3, Cp*). $^{11}B\{^1H\}$ NMR: −1.6 (2B), −2.6 (2B), −4.8 (3B), −6.5 (2B), −8.2 (1B). ^{13}C NMR: 8.36 (CH_3, Cp*), 8.87 (CH_3, Cp*), 8.97 (CH_3, Cp*), 9.18 (CH_3, Cp*), 22.07 (CH_2, Cp*), 88.20 (carborane), 92.44 (C, Cp*), 92.73 (C, Cp*), 93.48 (C, Cp*), 94.30 (C, Cp*), 95.53 (C, Cp*), 105.55 (CH, Ph), 106.17 (carborane), 110.56 (CH, Ph), 113.96 (C, Ph), 114.55 (CH, Ph), 116.73 (C, Ph), 120.33 (CH, Ph), 128.67 (CH, Ph), 134.43 (CH, Ph), 147.25 (C, Ph), 151.16 (C, Ph), 151.87 (C, Ph), 164.30 (C, Ph). ESI-MS (*m*/*z*): 807.25 (46%) $[M + H^+]^+$. IR (KBr, cm^{-1}): 2586.3 (ν_{B-H}). Anal. Found: C, 35.54; H, 4.01; N, 7.11. Calcd for $C_{24}H_{33}B_{10}IrN_4O_4S_2$: C, 35.76; H, 4.13; N, 6.95.

Preparation of complexes 7 and 8

The mixture of complex **2** (20.0 mg, 0.03 mmol) or **3** (20.0 mg, 0.03 mmol) and 1-azido-3-nitrobenzene (49.2 mg, 0.3 mmol) was heated in refluxing toluene for 24 hours. The solvent was removed and the crude product was purified by chromatography using silica gel to give a yellowish-brown solid **7** or **8**.

7 (8.6 mg, 35.6%). Yellowish-brown solid. ^1H NMR: 7.98 (d, *J* = 7.5 Hz, 1H, Ar*H*), 7.64 (d, *J* = 7.5 Hz, 1H, Ar*H*), 7.50 (t, *J* = 8.0 Hz, 1H, Ar*H*), 7.38 (d, *J* = 7.5 Hz, 1H, Ar*H*), 7.36 (d, *J* = 7.5 Hz, 1H, Ar*H*), 5.79 (t, *J* = 7.5 Hz, 1H, Ar*H*), 1.78 (s, 15H, CH_3, Cp*), 1.27 (s, 2H, CH_2). $^{11}B\{^1H\}$ NMR: −1.4 (2B), −2.6 (2B), −3.8 (2B), −7.0 (3B), −8.8 (1B). ^{13}C NMR: 9.05 (CH_3, Cp*), 32.99 (CH_2), 93.44 (carborane), 94.84 (C, Cp*), 97.21 (carborane), 103.43 (C, Ph), 107.62 (CH, Ph), 118.13 (CH, Ph), 119.87 (C, 4-nitro-3*H*-azepine), 128.84 (CH, 4-nitro-3*H*-azepine), 129.72 (C, 4-nitro-3*H*-azepine), 131.75 (CH, Ph), 133.19 (CH, 4-nitro-3*H*-azepine), 146.42 (CH, 4-nitro-3*H*-azepine), 148.94 (C, Ph), 162.89 (C, Ph). ESI-MS (*m*/*z*): 805.25 (100%) $[M]^-$. IR (KBr, cm^{-1}): 2574.2 (ν_{B-H}). Anal. Found: C, 35.59; H, 4.28; N, 6.72. Calcd for $C_{24}H_{33}B_{10}IrN_4O_4S_2$: C, 35.76; H, 4.13; N, 6.95.

8 (8.0 mg, 32.9%). Yellowish-brown solid. ^1H NMR: 8.01 (s, 1H, Ar*H*), 7.98 (d, *J* = 7.5 Hz, 1H, Ar*H*), 7.69 (d, *J* = 8.5 Hz, 1H, Ar*H*), 7.64 (d, *J* = 8.5 Hz, 1H, Ar*H*), 7.38 (d, *J* = 7.5 Hz, 1H, Ar*H*), 5.78 (t, *J* = 7.5 Hz, 1H, Ar*H*), 1.78 (s, 15H, CH_3, Cp*), 1.27 (s, 2H, CH_2). $^{11}B\{^1H\}$ NMR: −1.2 (2B), −2.5 (2B), −4.4 (2B), −7.0 (3B), −9.8 (1B). ^{13}C NMR: 9.16 (CH_3, Cp*), 32.19 (CH_2),

Table 1 Selected bond lengths (Å) and angles (°) for **2–4** and **6–8**

	2	3	4	6	7	8
Ir1–S1	2.364(2)	2.3706(14)	2.2596(16)	2.3708(17)	2.3724(15)	2.3622(12)
Ir1–S2	2.311(2)	2.3087(13)	2.2667(13)	2.3139(13)	2.2769(14)	2.2953(11)
Ir1–N1	2.045(8)	2.066(3)		2.051(4)	2.168(4)	2.125(4)
N1–C13	1.349(13)	1.330(6)		1.343(7)	1.393(5)	1.395(4)
C1–C2	1.649(12)	1.680(6)	1.631(7)	1.669(8)	1.693(10)	1.667(5)
S1–C1	1.786(10)	1.777(4)	1.793(5)	1.771(4)	1.783(6)	1.769(5)
S2–C2	1.847(8)	1.821(4)	1.800(5)	1.830(6)	1.824(6)	1.824(5)
S2–C14	1.766(10)	1.764(4)		1.730(4)	1.784(3)	1.776(4)
S1–Ir1–S2	91.55(8)	91.91(4)	92.35(5)	91.49(5)	91.79(5)	91.75(4)
S1–Ir1–N1	87.3(2)	89.14(10)		87.69(14)	88.07(12)	87.08(10)
S2–Ir1–N1	82.3(2)	81.72(10)		82.46(12)	81.44(12)	82.10(11)
Ir1–S1–C1	104.2(3)	105.24(13)	107.16(17)	104.6(2)	105.3(2)	105.06(12)
Ir1–S2–C2	105.2(3)	106.28(14)	106.34(16)	106.16(17)	108.5(2)	107.28(15)
Ir1–S2–C14	100.7(3)	100.00(15)		99.87(16)	100.69(11)	99.31(14)
Ir1–N1–C13	121.8(6)	120.2(3)		121.1(4)	113.3(3)	115.9(3)
C2–S2–C14	103.8(4)	104.7(2)		104.1(2)	103.0(2)	104.20(19)
S1–C1–C2	119.2(6)	118.7(3)	116.6(3)	119.6(4)	119.3(4)	120.0(3)
S2–C2–C1	116.7(6)	117.1(3)	117.5(3)	116.2(3)	115.0(4)	115.6(3)
N1–C13–C14	119.1(9)	120.2(4)		118.1(5)	119.9(3)	118.4(4)
S2–C14–C13	115.4(7)	115.3(3)		116.9(4)	115.9(2)	117.6(3)

Table 2 Crystallographic data for **2–4** and **6–8**

Compound	**2**	**3**	**4**	**6**	**7**	**8**
Chemical formula	$C_{18}H_{29}B_{10}IrN_2O_2S_2$	$C_{18}H_{29}B_{10}IrN_2O_2S_2$	$C_{18}H_{29}B_{10}IrN_2O_2S_2$	$2(C_{24}H_{33}B10IrN_4O_4S_2)\cdot2(C_4H_{10}O)\cdot H_2O$	$2(C_{24}H_{33}B_{10}IrN_4O_4S_2)\cdot2H_2O$	$C_{24}H_{33}B_{10}IrN_4O_4S_2$
Formula weight	669.89	669.85	669.89	1778.18	1647.95	806.00
Crystal size (mm)	0.25 × 0.28 × 0.32	0.22 × 0.26 × 0.28	0.19 × 0.23 × 0.28	0.22 × 0.24 × 0.28	0.22 × 0.24 × 0.28	0.17 × 0.20 × 0.22
Temperature (K)	296(2)	296(2)	296(2)	291(2)	291(2)	296(2)
Radiation	0.71073	0.71073	0.71073	0.71073	0.71073	0.71073
Crystal system	Triclinic	Monoclinic	Triclinic	Monoclinic	Monoclinic	Monoclinic
Space group	$P\bar{1}$	$P2(1)/c$	$P\bar{1}$	$P2(1)/n$	$P2(1)/n$	$P21/c$
a (Å)	11.5068(13)	10.609(3)	11.7159(13)	15.1459(17)	22.174(4)	11.0515(11)
b (Å)	11.6106(13)	19.715(6)	14.4682(16)	19.412(2)	11.138(2)	15.1858(14)
c (Å)	11.7113(13)	13.552(4)	17.9172(19)	15.4035(17)	29.537(6)	21.9777(17)
α (°)	65.2490(10)	90.00	69.271(2)	90.00	90.00	90.00
β (°)	67.5340(10)	110.844(4)	72.654(2)	117.8850(10)	106.161(4)	120.189(3)
γ (°)	84.9640(10)	90.00	72.994(2)	90.00	90.00	90.00
V (Å^3)	1308.2(3)	2649.0(14)	2651.2(5)	4002.9(8)	7007(2)	3188.2(5)
Z	2	4	4	2	4	4
ρ_{calc} (g cm^{-3})	1.701	1.680	1.678	1.475	1.561	1.679
F (000)	652	1304	1304	1772	3244	1584
Absorp. coeff. (mm^{-1})	5.284	5.219	5.214	3.481	3.970	4.358
θ Range (°)	1.92 to 26.00	1.91 to 26.00	1.24 to 26.00	1.83 to 26.00	1.02 to 26.00	1.72 to 25.67
Reflns collected	7205 (R_{int} = 0.1303)	14 363 (R_{int} = 0.0462)	16 254 (R_{int} = 0.0332)	21 404 (R_{int} = 0.0403)	40 678 (R_{int} = 0.0411)	14 165 (R_{int} = 0.0282)
Indep. reflns	5029	5201	10 376	7858	13 753	6050
Refns obs. [$I > 2\sigma(I)$]	4639	3809	8603	5929	10 757	4879
Data/restr/paras	5029/0/321	5201/0/321	10 376/26/658	7858/3/472	13 753/0/850	6050/0/411
GOF	1.039	0.981	1.063	1.049	1.061	1.004
R_1/wR_2 [$I > 2\sigma(I)$]	0.0601/0.1613	0.0274/0.0416	0.0344/0.0871	0.0396/0.0920	0.0414/0.0888	0.0284/0.0609
R_1/wR_2 (all data)	0.0621/0.1630	0.0462/0.0432	0.0428/0.0909	0.0550/0.0967	0.0560/0.0941	0.0399/0.0639
Large peak and hole (e Å^{-3})	2.698/−4.814	1.026/−0.958	2.217/−1.544	0.624/−1.202	0.659/−1.040	0.866/−0.500

92.72 (carborane), 94.87 (C, Cp*), 96.02 (carborane), 107.78 (CH, Ph), 115.09 (CH, Ph), 117.17 (CH, 4-nitro-3*H*-azepine), 117.32 (C, Ph), 119.15 (C, 4-nitro-3*H*-azepine), 129.32 (C, 4-nitro-3*H*-azepine), 131.36 (CH, 4-nitro-3*H*-azepine), 134.41 (CH, Ph), 145.93 (CH, 4-nitro-3*H*-azepine), 150.54 (C, Ph), 160.13 (C, Ph). ESI-MS (*m*/*z*): 805.33 (100%) $[M]^-$. IR (KBr, cm^{-1}): 2587.9 (ν_{B-H}). Anal. Found: C, 35.48; H, 4.04; N, 6.81. Calcd for $C_{24}H_{33}B_{10}IrN_4O_4S_2$: C, 35.76; H, 4.13; N, 6.95.

X-ray crystal structure determinations

Crystals suitable for X-ray analysis were obtained by the slow evaporation of a solution in petroleum ether–dichloromethane. Diffraction data were collected using a Bruker SMART Apex II CCD diffractometer by means of graphite monochromated MoKα (λ = 0.71073 Å) radiation. During collection of the intensity data, no significant decay was observed. The intensities were corrected for Lorentz polarization effects and empirical absorption by using the SADABS program.[29] The structures were solved by direct methods with the SHELXS-97 program[30] and were refined on F^2 with SHELXTL (version 6.14).[31] All non-hydrogen atoms were refined anisotropically. Hydrogen atoms were included in calculated positions and were refined using a riding model. A summary of selected bond lengths and angles, crystallographic data and details of data collection and structure refinements of complexes **2–4** and **6–8** is provided in Tables 1 and 2 and CIF files (CCDC no. 936371–936376).

Acknowledgements

This work was supported by the National Basic Research Program of China (2010CB923303 and 2013CB922101), the National Science Foundation of China (20925104, 21271102 and 21021062) and NSFC-RFBR joint grant (21110143 and 12-03-91165).

Notes and references

1 C. Wentrup, *Acc. Chem. Res.*, 2011, **44**, 393–404.
2 T. G. Driver, *Org. Biomol. Chem.*, 2010, **8**, 3831–3846.
3 S. Bräse, C. Gil, K. Knepper and V. Zimmermann, *Angew. Chem., Int. Ed.*, 2005, **44**, 5188–5240.
4 N. P. Gritsan and M. S. Platz, *Chem. Rev.*, 2006, **106**, 3844–3867.
5 M. L. Tsao and M. S. Platz, *J. Am. Chem. Soc.*, 2003, **125**, 12014–12025.
6 D. Grote and W. Sander, *J. Org. Chem.*, 2009, **74**, 7370–7382.
7 C. Carra, R. Nussbaum and T. Bally, *ChemPhysChem*, 2006, **7**, 1268–1275.
8 R. Warmuth and S. Makowiec, *J. Am. Chem. Soc.*, 2007, **129**, 1233–1241.
9 R. A. Eikey and M. M. Abu-Omar, *Coord. Chem. Rev.*, 2003, **243**, 83–124.
10 S. Cenini, E. Gallo, A. Caselli, F. Ragaini, S. Fantauzzi and C. Piangiolino, *Coord. Chem. Rev.*, 2006, **250**, 1234–1253.
11 D. E. Wigley, *Prog. Inorg. Chem.*, 2007, **42**, 239–482.
12 M. M. Abu-Omar, C. E. Shields, N. Y. Edwards and R. A. Eikey, *Angew. Chem., Int. Ed.*, 2005, **44**, 6203–6207.
13 V. Lyaskovskyy, A. I. O. Suarez, H. Lu, H. Jiang, X. P. Zhang and B. de Bruin, *J. Am. Chem. Soc.*, 2011, **133**, 12264–12273.
14 A. Takaoka, M.-E. Moret and J. C. Peters, *J. Am. Chem. Soc.*, 2012, **134**, 6695–6706.
15 G. Bucher, C. Tönshoff and A. Nicolaides, *J. Am. Chem. Soc.*, 2005, **127**, 6883–6892.
16 N. P. Gritsan, I. Likhotvorik, M.-L. Tsao, N. Çelebi, M. S. Platz, W. L. Karney, C. R. Kemnitz and W. T. Borden, *J. Am. Chem. Soc.*, 2001, **123**, 1425–1433.
17 P. G. S. Dkhar and R. H. D. Lyngdoh, *J. Mol. Struct. (THEOCHEM)*, 2005, **732**, 161–171.
18 J. Xue, H. L. Luk, S. V. Eswaran, C. M. Hadad and M. S. Platz, *J. Phys. Chem. A*, 2012, **116**, 5325–5336.
19 X. Meng, F. S. Wang and G. X. Jin, *Coord. Chem. Rev.*, 2010, **254**, 1260–1272.
20 W. Zhong, M. Xie, Q. Jiang, Y. Li and H. Yan, *Chem. Commun.*, 2012, **48**, 2152–2154.
21 M. Herberhold, H. Yan, W. Milius and B. Wrackmeyer, *Angew. Chem., Int. Ed.*, 1999, **38**, 3689–3691.
22 B. H. Xu, X. Q. Peng, Y. Z. Li and H. Yan, *Chem.–Eur. J.*, 2008, **14**, 9347–9356.
23 B. H. Xu, J. C. Tao, Y. Z. Li, S. H. Li and H. Yan, *Organometallics*, 2008, **27**, 334–340.
24 H. D. Ye, G. Y. Ding, M. S. Xie, Y. Z. Li and H. Yan, *Dalton Trans.*, 2011, **40**, 2306–2313.
25 E. Kumaran, V. S. Sridevi and W. K. Leong, *Organometallics*, 2010, **29**, 6417–6421.
26 A. Houmam, *Chem. Rev.*, 2008, **108**, 2180–2237.
27 J. Y. Bae, Y. I. Park, J. Ko, K. I. Park, S. I. Cho and S. Ook Kang, *Inorg. Chim. Acta*, 1999, **289**, 141–148.
28 L. Dyall, *Aust. J. Chem.*, 1986, **39**, 89–101.
29 G. M. Sheldrick, *SADABS, A Program for Empirical Absorption Correction*, University of Göttingen, Germany, 1998.
30 G. M. Sheldrick, *SHELXL-97, Program for the Refinement of Crystal Structures*, University of Göttingen, Germany, 1997.
31 G. M. Sheldrick, *Acta Crystallogr., Sect. A: Fundam. Crystallogr.*, 2008, **64**, 112–122.

